MICROSCOPY RESEARCH AND TECHNIQUE 37:229–241 (1997)

Ultrastructural Characterization of Sulfur Mustard–Induced Vesication in Isolated Perfused Porcine Skin

NANCY A. MONTEIRO-RIVIERE* AND ALFRED O. INMAN
Cutaneous Pharmacology and Toxicology Center, North Carolina State University, Raleigh, North Carolina 27606

KEY WORDS: microvesicle; blisters; sulfur mustard (bis(2-chloroethyl) sulfide); isolated perfused skin; vesication; histology; in vitro; skin; toxicology; pig; ultrastructure

ABSTRACT The isolated perfused porcine skin flap (IPPSF) is a novel alternative, humane in vitro model consisting of a viable epidermis and dermis with a functional microvasculature. For this study, 200 µl of either 10.0, 5.0, 2.5, 1.25, 0.50, or 0.20 mg/ml of bis (2-chloroethyl) sulfide (HD) in ethanol or ethanol control was topically applied to a 5.0 cm^2 dosing area of the IPPSF and perfused for 8 h with recirculating media. HD dermatotoxicity was assessed in the flap by cumulative glucose utilization (CGU), vascular resistance (VR), light microscopy (LM), scanning electron microscopy (SEM), and transmission electron microscopy (TEM). HD produced a statistically significant dose relationship for gross blisters and microvesicles. The HD-treated IPPSFs were also characterized by a decrease in CGU and an increase in VR. Light microscopic changes included mild intracellular and slight intercellular epidermal edema, multifocal epidermal-dermal separation, and dark basal cells. Ultrastructural alterations consisted of cytoplasmic vacuoles, pyknotic basal cells, nucleolar segregation, and epidermal-dermal separation occurring between the lamina lucida and lamina densa of the basement membrane. The severity of these changes increased in a dose-dependent manner. Morphologically, the IPPSF appeared similar to human skin exposed to HD with the formation of macroscopic blisters and microscopic vesicles. In conclusion, the IPPSF appears to be an appropriate in vitro model with which to study the pathogenesis of vesicant-induced toxicity. *Microsc. Res. Tech., 37:229–241, 1997.*

INTRODUCTION

The mechanism of cutaneous vesication has eluded investigators since chemical vesicants were first deployed in World War I. With the recent use of sulfur mustard (bis (2-chloroethyl) sulfide [HD]) in the Iran-Iraq war, interest has been renewed to determine the biochemical basis of agent-induced cutaneous vesication. Part of the problem resides in the model systems used to study these events. HD is a lipophilic compound which penetrates the skin to cause erythema and blistering after a 4–24 h latency period. In the presence of water, HD hydrolyzes to form hydrochloric acid and thiodiglycol. Humans exposed to the topical vesicant HD, after a delay of a few hours, usually develop fluid-filled blisters which require a prolonged period to heal (Renshaw, 1946; Requena et al., 1988; Willems, 1989). Although in vivo exposure to HD causes some animals to form gross blisters, the experimental end point is often the histological evidence of microvesicles. Since gross blisters never form with in vitro human and animal models, microvesicles are usually the accepted toxicologic end point. Part of this discrepancy is undoubtedly a result of the complex pathogenesis of chemical vesication. The initiating biochemical lesion (DNA alkylation, glutathione depletion, inhibition of glycolysis, alkylation of basement membrane molecules) may be studied in vitro, but the formation of gross blisters probably requires other physiological factors not present in simple in vitro skin models. Although in vivo models may produce the relevant lesions, mechanistic studies are difficult to conduct, and the humane aspects of animal exposure preclude their widespread use.

The isolated perfused porcine skin flap (IPPSF) is a novel in vitro animal model utilized to study percutaneous absorption of a number of drugs and chemicals (Riviere and Monteiro-Riviere, 1991; Riviere et al., 1991; Williams et al., 1990). This system provides the major advantage of a viable, full-thickness skin preparation with an intact vasculature, a relatively large surface area for dosing, and control over experimental parameters and sample collection. Since pig skin is a well-accepted model for percutaneous absorption studies (Bartek et al., 1972; Reifenrath et al., 1984a; 1984b; Wester and Maibach, 1985), the IPPSF should also be an excellent alternative animal model for investigating cutaneous toxicity. This has been demonstrated with a series of studies using various topically applied chemicals (Riviere et al., 1991; Williams et al., 1990). Studies with the HD monofunctional analogue 2-chloroethyl methyl sulfide (CEMS) (King and Monteiro-Riviere, 1990) and lewisite (L) (King et al., 1992) demonstrated that the IPPSF produced gross fluid-filled blisters following exposure. Transmission electron microscopy revealed separation between the lamina lucida and

Received 15 April 1995; Accepted in revised form 15 July 1995.

Contract grant sponsor: U.S. Army Medical Research and Development Command; Contract grant number: DAMD 17-87C-7139.

*Correspondence to Nancy A. Monteiro-Riviere, Cutaneous Pharmacology and Toxicology Center, North Carolina State University, 4700 Hillsborough St., Raleigh, NC 27606. Email: Nancy_Monteiro@NCSU.EDU

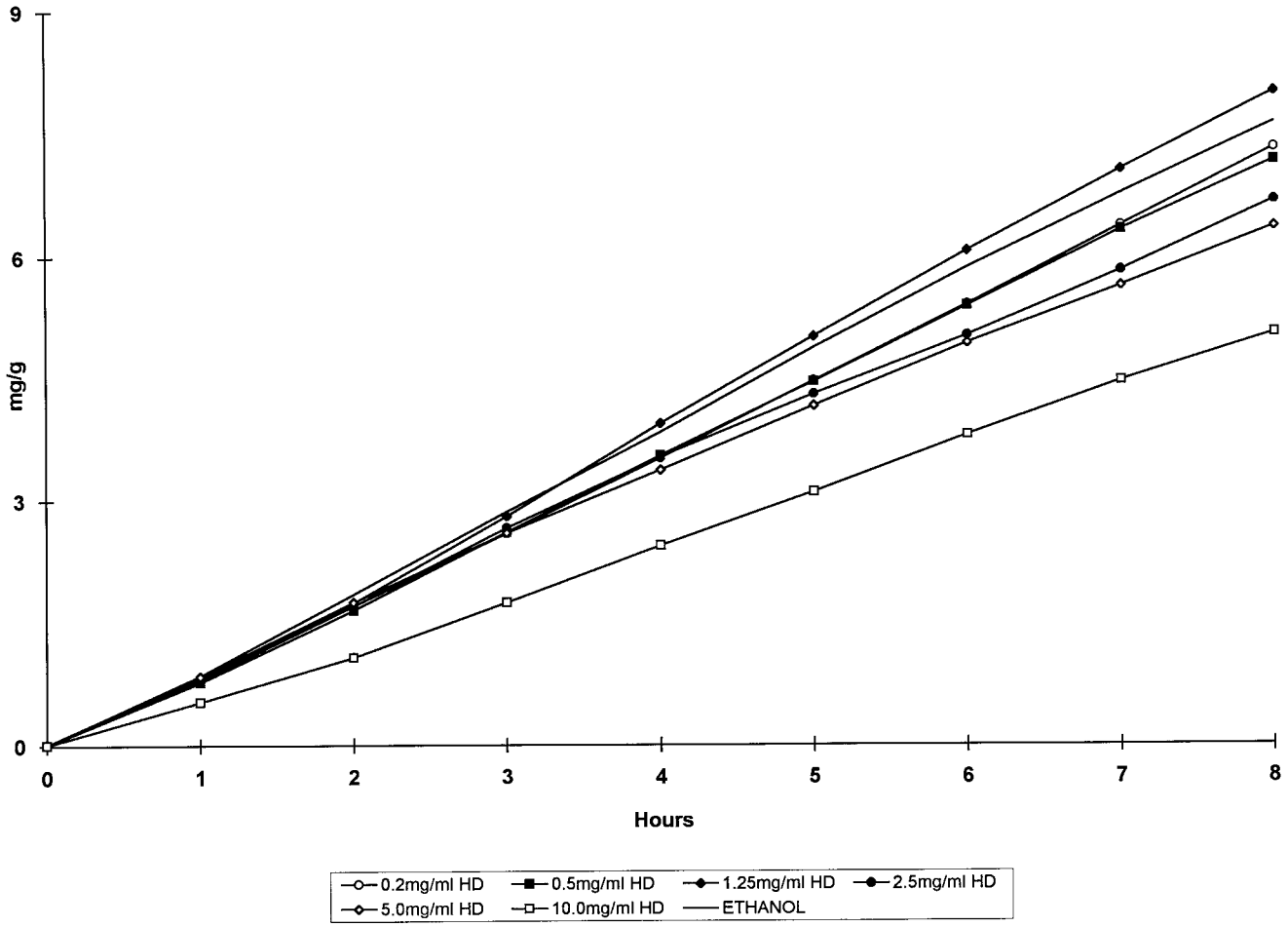

Fig. 1. Plot illustrating CGU of HD treatments and ethanol control.

lamina densa in the epidermal-dermal junction (EDJ), with intracellular vacuolization and mitochondrial swelling in the stratum basale and stratum spinosum cells. These changes were similar to those described after human exposure to sulfur mustard (Renshaw, 1946; Requena et al., 1988). Since the IPPSF has been utilized to predict in vivo human chemical percutaneous absorption (Riviere and Monteiro-Riviere, 1991), the absorptive phase in the pathogenesis of agent-induced vesication can also be modeled. Thus, it appears that the IPPSF may be ideal to study the mechanism of HD vesication since its biological complexity falls between the simpler in vitro systems and the complex in vivo setting.

The purpose of this study was to investigate the pathogenesis of HD-induced vesication by characterizing the biochemical, physiological, and morphological responses in the IPPSF and determine the optimal vesicating dose.

MATERIALS AND METHODS

IPPSF Preparation and Dosing Protocol

Female Yorkshire weanling pigs weighing 20–30 kg were purchased commercially and acclimated for 1 week prior to surgery. The pigs were housed in a temperature (22°C) and light/dark- (12 h/12 h) regulated facility on elevated pen floors and provided ad libitum with water and 15% protein pig and sow pellets (Wayne Feeds Division, Chicago, IL). The surgical procedure involved the creation of two single-pedicle, axial pattern, island tubed skin flaps each lateral to the ventral midline on the pig abdomen (Bowman et al., 1991; Carver et al., 1989; Monteiro-Riviere, 1990a; Monteiro-Riviere et al., 1987; Riviere et al., 1986). Each flap was created during stage I and harvested 48 h later during stage II surgery. The flaps were then cannulated, flushed with heparinized saline to clear the vasculature of blood, and transferred to the perfusion chamber maintained in a specially designed fume hood for chemical agents.

Each flap was perfused with 300 ml of a recirculated medium consisting of a modified Krebs-Ringer bicarbonate buffer (pH 7.4, 350 mOsm/kg) containing bovine serum albumin (45 g/l) and glucose (80–120 mg/dl) as the primary energy source. The temperature (37°C) and humidity (60–80%) in the chamber and the media flow rate (1.5 ml/min) were monitored and remained constant throughout the entire perfusion period. In addition, the media was gassed with 95% oxygen and 5% carbon dioxide via a silastic oxygenator. Since the IPPSF is not a sterile organ preparation, antimicrobials (penicillin G and amikacin) were added to the media to

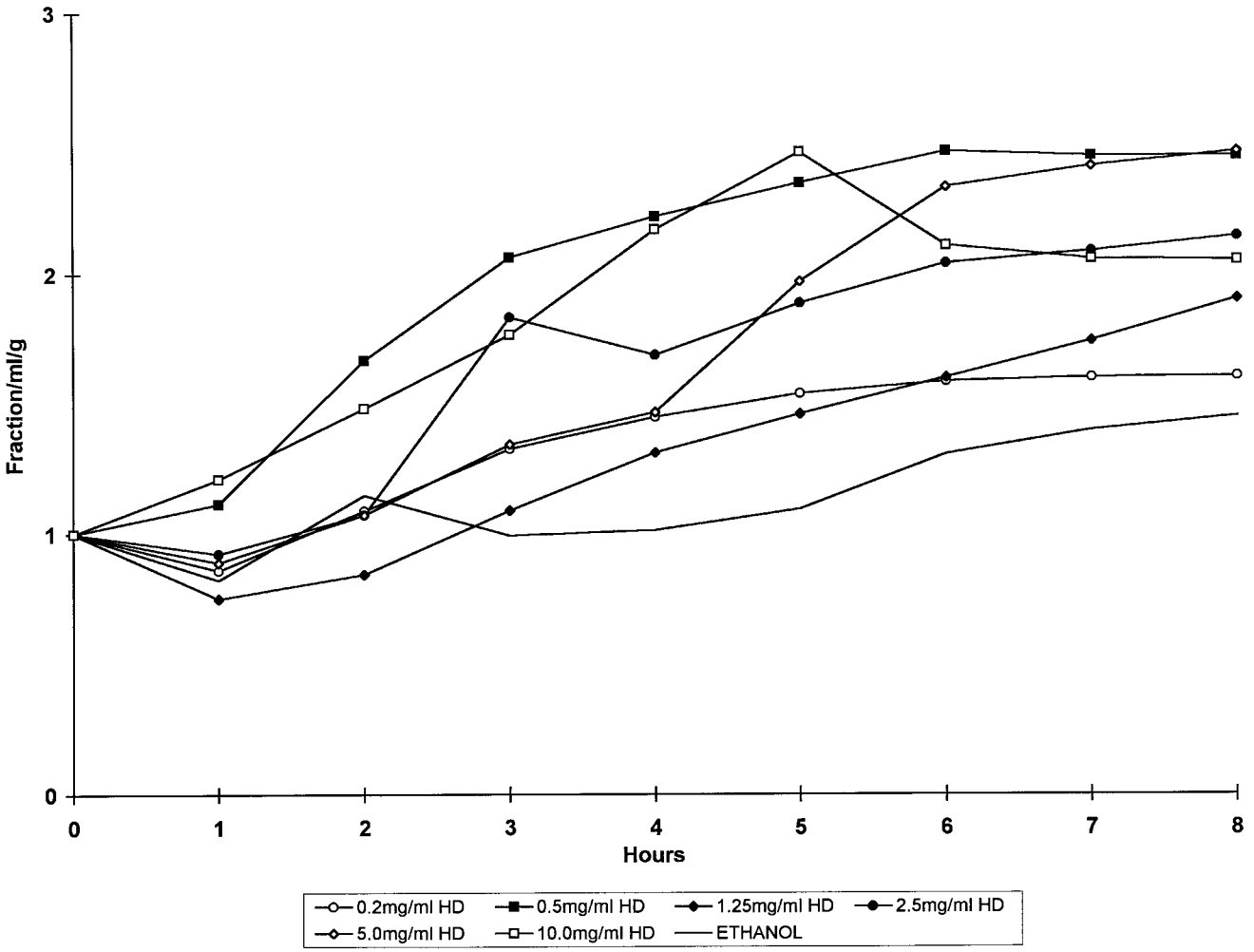

Fig. 2. Plot illustrating vascular resistance for HD treatments and ethanol control.

TABLE 1. Frequency of morphological lesions noted with HD exposure

Treatment	Blisters	Microvesicles
10.00 mg/ml	4/5	5/5
5.00 mg/ml	2/4	3/4
2.50 mg/ml	1/4	2/4
1.25 mg/ml	0/3	2/3
0.50 mg/ml	1/3	1/3
0.20 mg/ml	1/4	1/4

prevent bacterial overgrowth from the microflora normally present on the skin surface. Heparin was included to prevent coagulation from residual blood elements in the vasculature of the flap.

Each IPPSF was perfused for 1 h prior to dosing to assess biochemical (glucose utilization) and morphological viability. Twenty-nine flaps were used in this dose-response study to determine the dose that would produce a lesion of specific severity. The IPPSFs were dosed with 200 µl of either 10.0 mg/ml (n = 5), 5.0 mg/ml (n = 4), 2.5 mg/ml (n = 4), 1.25 mg/ml (n = 3), 0.5 mg/ml (n = 3), or 0.2 mg/ml (n = 4) HD in ethanol within a 5.0 cm^2 flexible (Stomahesive; Convatec-Squibb, Princeton, NJ) template using a Microman pipette (Gilson Medical Electronics S.A., Villers-le-Bel, France). This pipette system offers disposable pipette tips and plungers for the immediate decontamination of the dosing system and preventing HD contamination between flaps. Additional flaps (n = 4) were treated with ethanol and served as controls.

Biochemical and Vascular Parameters

Hourly samples were taken of the arterial medium and the venous effluent and analyzed for glucose content. Cumulative glucose utilization (CGU) has been used as an indicator of biochemical viability (Carver et al., 1989; King and Monteiro-Riviere, 1990, 1991; King et al., 1992; Monteiro-Riviere, 1990a,b; Riviere et al., 1986, 1987). These parameters were used to determine the biochemical effects of HD on IPPSF metabolism and to evaluate IPPSF viability. Hourly glucose utilization (GU) was used as the sole parameter of biochemical viability prior to dosing, with a value less than 10 mg/h/IPPSF or a plateau in the upward slope of CGU indicating a loss of viability in the skin flap preparation. The vascular response of the IPPSF was characterized using the physiological parameter vascular resistance (VR) (pressure/flow). This parameter was normalized to an individual flap basis by dividing by

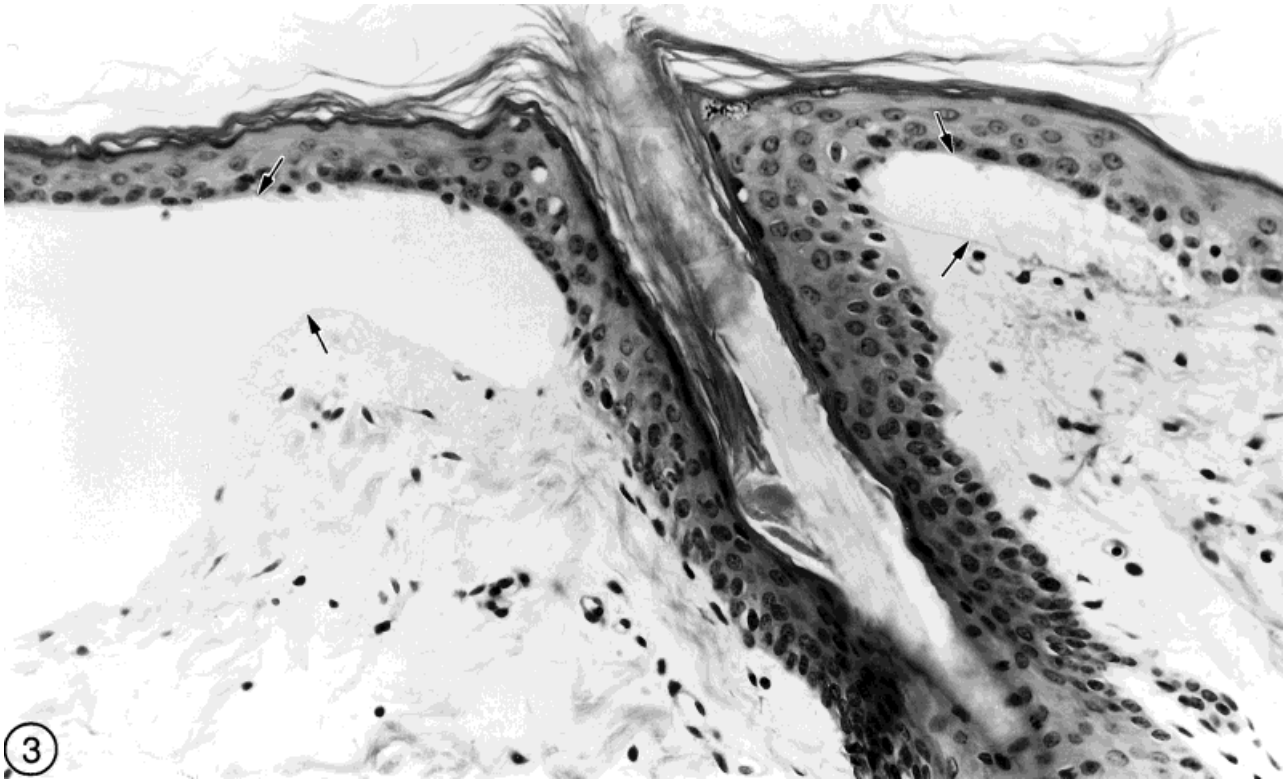

Fig. 3. LM of a 0.2 mg/ml of HD-treated IPPSF depicting epidermal-dermal separation (arrows) on either side of the hair follicle. H&E. ×350.

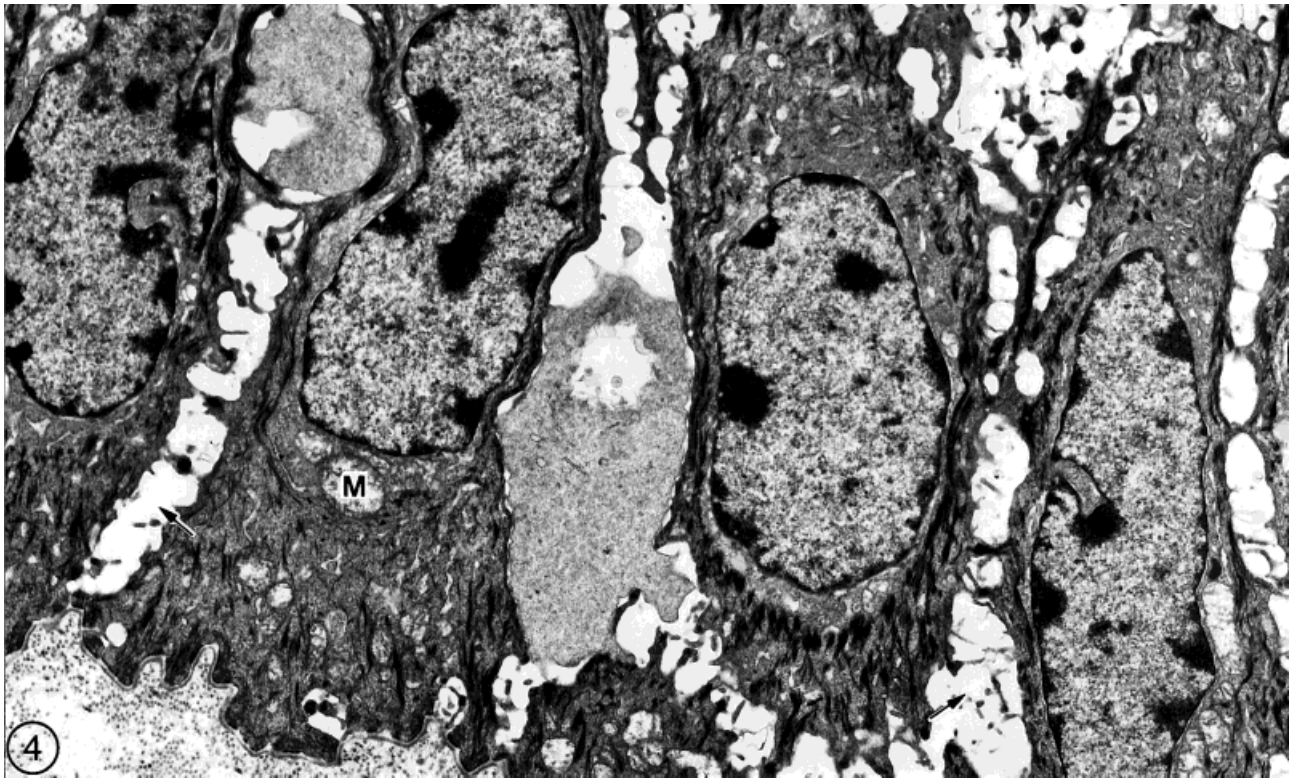

Fig. 4. TEM of a 0.2 mg/ml of HD-treated IPPSF depicting intercellular edema (arrows) and blown-out mitochondria (M) in the stratum basale layer. ×7,200.

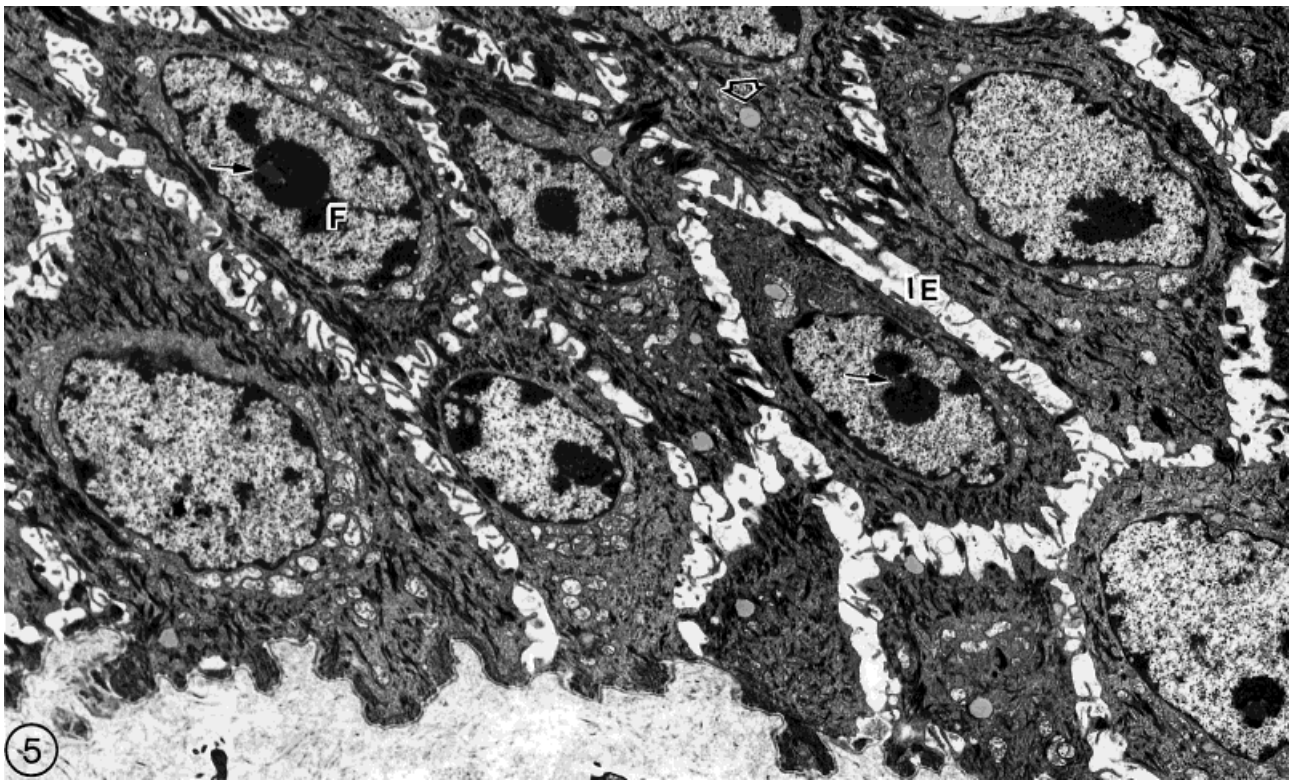

Fig. 5. TEM of 0.5 mg/ml of HD-treated IPPSF showing slight intercellular epidermal edema (IE) and lipid inclusions (open arrow). Note nuclei with enlarged granular structures (arrows) surrounded by a dense fibrillar component (F). Nucleolar margination and nucleolar caps are present in adjacent cells. ×4,700.

the initial VR value in order to obtain a plot of fractional VR to compensate for initial differences between IPPSFs' baseline VR.

Tissue Preparation and Morphological Parameters

Following flap perfusion, the skin within the entire dose area was excised and tissue samples taken for light microscopy (LM), scanning electron microscopy (SEM), and transmission electron microscopy (TEM). LM samples were fixed in cold (4°C) 10% neutral buffered formalin, processed routinely, and embedded in paraffin. Tissue was sectioned at 6 µm, stained with hematoxylin and eosin (H&E) or periodic acid–Schiff (PAS), and viewed on an Olympus BH-2 photomicroscope (Olympus Optical, Ltd., Tokyo, Japan). TEM samples were trimmed, fixed in cold (4°C) half-strength Karnovsky's fixative (2.0% paraformaldehyde, 2.5% glutaraldehyde in 0.1 M cacodylate buffer, pH 7.2) for 24 h (Monteiro-Riviere and Manning, 1987), postfixed in 1% osmium tetroxide, dehydrated through a graded series of ethanols, infiltrated, and embedded in Spurr's resin. Thick sections (approximately 1 µm) were stained with 1% toluidine blue for orientation and localization of lesions. Thin sections (800–1000 Å) were mounted on copper grids, poststained with uranyl acetate and lead citrate, and examined on a Philips EM410 LS transmission electron microscope (Philips Electronics, Mahway, NJ) operating at an accelerating voltage of 80 KV. For SEM, tissues were fixed in 4% paraformaldehyde and 1% glutaraldehyde in phosphate buffer overnight at 4°C (McDowell and Trump, 1976). Specimens were postfixed in 1% osmium tetroxide in 0.1 M phosphate buffer, dehydrated through graded ethanol solutions, and critical-point-dried in 100% ethanol. They were then mounted on aluminum stubs and sputter-coated (Hummer VI, Anatech, Ltd.) with gold-palladium. Tissue samples were examined on a JEOL JSM 35 CF (JEOL, LTD, Tokyo, Japan) scanning electron microscope operating at 15 KV.

Statistical Comparisons

Statistical comparisons of the CGU between treatments was performed by calculating the average rate of change over the time course of perfusion (slope). Statistical comparison of VR was performed between treatment means of each dose as well as at each specific time point. Differences between treatments were analyzed by the general linear model procedure (SAS Institute Inc., Cary, NC), while multiple comparison tests were performed using the Student's (least significant differences) *t*-test for type I comparison-wise error.

RESULTS

Biochemical and Physiological Parameters

CGU was used to determine the effects of HD on the viability of the flap. The mean CGU of all treatments increased in a linear manner (Fig. 1). Terminal CGU values were greatest in the 1.25 mg/ml dose, followed by the ethanol control, 0.2, 0.5, 2.5, and 5.0 mg/ml dosed flaps. The 10.0 mg/ml flaps demonstrated the most dramatic decrease in CGU when compared to controls. Statistical comparison of CGU slopes showed signifi-

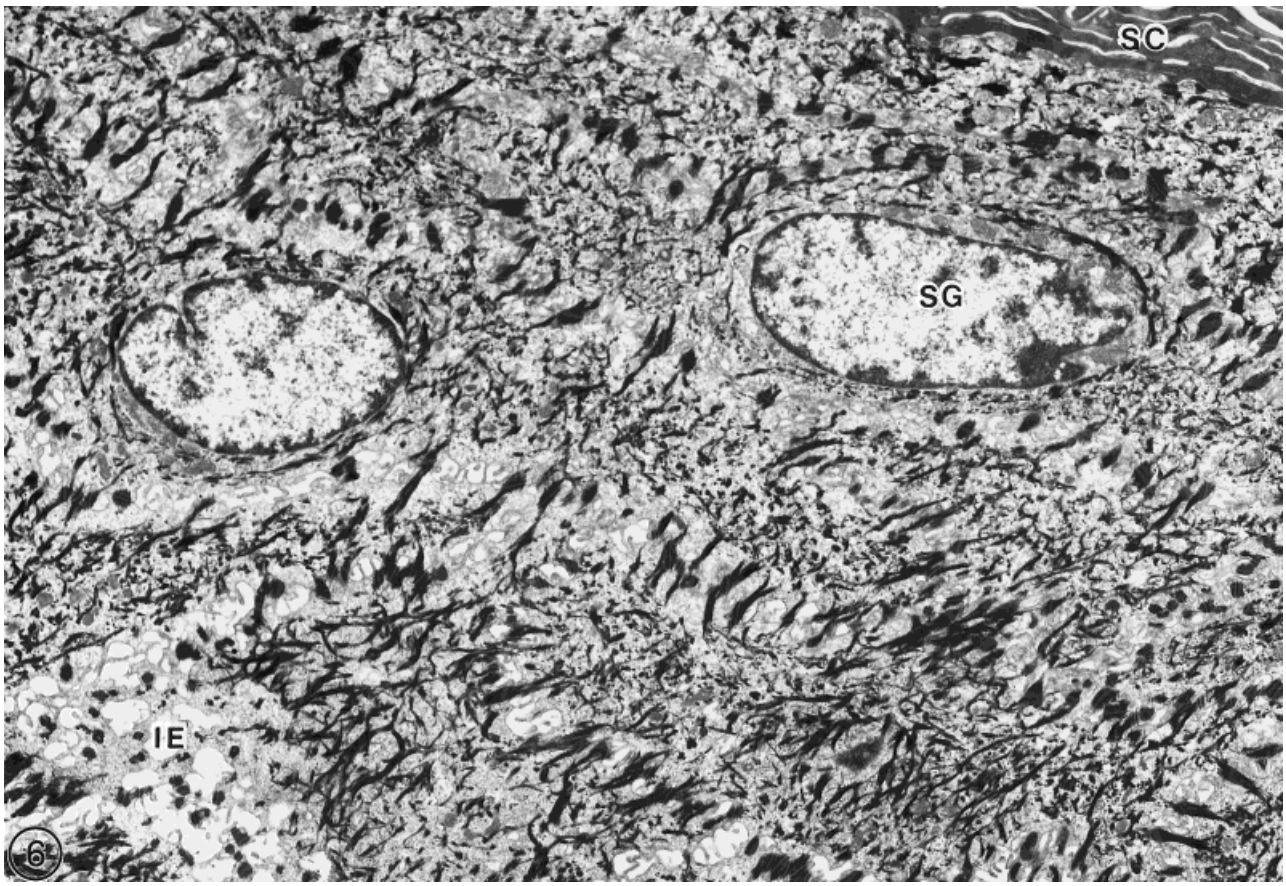

Fig. 6. TEM of a 1.25 mg/ml of HD-treated IPPSF depicting normal stratum granulosum (SG) and stratum corneum (SC) layers. Note slight intercellular edema (IE). ×6,000.

cant differences ($P < 0.05$) between the 10.0 mg/ml dose and the 1.25, 0.2, and 0.5 mg/ml doses.

VR was used to assess the vascular activity of each dose on the IPPSF. One hour following dose, all treatments, except the ethanol controls, showed an increase in mean VR (Fig. 2). In the controls, VR remained steady from 1–8 h. Significant differences were found between the treatment means of the 1.25 mg/ml dose and 0.5, 5.0, and 10.0 mg/ml doses. Also, differences were present between the 0.2 mg/ml dose and the 0.5 and 10.0 mg/ml doses and between the controls and all dosed treatments. The time-wise comparison of VR shows some significant differences between ethanol and dosed treatments. From 6–8 h postdose, the 0.5, 2.5, 5.0, and 10.0 mg/ml dosed treatments were significantly different ($P < 0.05$) from the ethanol controls.

Morphology

Table 1 summarizes the presence of blisters at each HD dose. Gross blisters, which usually appeared near the end of the perfusion period, were filled with a clear fluid and raised above the skin surface. Macroscopic and microscopic observations of HD-treated flaps showed a dose-related effect in the IPPSF.

LM of the 0.2 mg/ml of HD-treated IPPSFs consistently had mild intracellular and intercellular epidermal edema. The IPPSF that had blistered at 0.2 mg/ml of HD showed focal basement membrane separation between the epidermis and the dermis with only a few pyknotic cells (Fig. 3). TEM of the 0.2 mg/ml–treated IPPSFs that did not blister demonstrated slight intercellular epidermal edema, mild intracellular edema (hydropic degeneration), blown-out mitochondria, and typical nucleolar pleomorphism, while the epidermal-dermal junction appeared normal (Fig. 4). LM of the 0.5 mg/ml of HD flaps showed slight intracellular and intercellular epidermal edema. TEM showed a normal epidermal-dermal junction, lipid inclusions in the stratum basale cells, and nuclear and nucleolar segregation which formed an unusual pattern (Fig. 5). At times, the center of the nucleolus had an enlarged fibrous center with an adjacent granular and dense filamentous component (Figure 5).

Light microscopy of the 1.25 mg/ml of HD-treated IPPSFs demonstrated a normal stratum corneum, slight hydropic degeneration, and intercellular edema with some focal spongiotic vesicles. Only one flap showed slight pyknotic basal cells. TEM showed a normal basement membrane in the nonblistered flap, with normal stratum basale, stratum spinosum, stratum granulosum, and stratum corneum cells (Fig. 6). LM of the IPPSFs treated with 2.5 mg/ml of HD showed intracellular and slight intercellular epidermal edema. A few pyknotic, dyskeratotic, and karyolytic stratum basale cells were present. TEM of the basement membrane in the nonblistered flaps appeared normal. Also, a few lipid inclusion bodies were seen in some cells along with ruptured mitochondria without cristae and

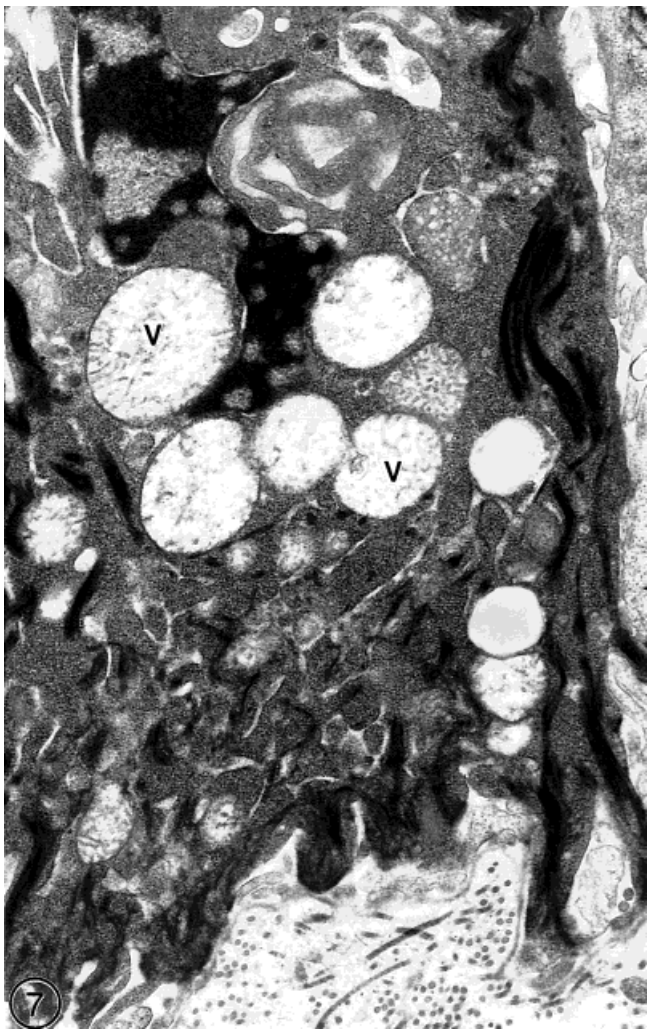

Fig. 7. TEM of a 2.5 mg/ml of HD-treated IPPSF showing a degenerative dark basal cell containing large cytoplasmic vacuoles (V). ×16,500.

nuclear envelope separation. Large cytoplasmic vacuoles containing cellular debris, probably the remnants of damaged mitochondria, were present in the degenerative stratum basale cells (Fig. 7).

The 5.0 mg/ml HD-treated flaps showed a moderate amount of pyknosis in the stratum basale cells. Hydropic degeneration was severe and so extensive that it led to reticular degeneration in some IPPSFs. The severity of this liquefaction degeneration probably resulted in the multiple focal areas of moderate (5–20 cells affected) epidermal-dermal separation (Fig. 8). Also, intercellular edema (spongiosis) and dyskeratotic and karyolytic basal cells were more numerous than at the lower concentrations of HD. All of these lesions were focal, where one area may appear normal and yet adjacent areas may exhibit separation of the epidermis and dermis. TEM of a 5.0 mg/ml–treated IPPSF showed numerous damaged mitochondria in both the stratum basale and stratum spinosum layers. Mitochondria became so edematous that they eventually merged and coalesced, thereby forming a large crescent-shaped vacuole containing cristae debris which may correspond to the paranuclear vacuoles (Fig. 9).

The morphological effects in the highest dose of HD were more severe than in the previous doses. All but one of the 10.0 mg/ml HD-treated IPPSFs showed macroscopic blisters, while all had microvesicles. LM evaluation of these flaps showed intracellular edema (hydropic degeneration or liquefaction degeneration), slight intercellular edema, focal epidermal necrosis, pyknotic basale cells, and severe epidermal-dermal separation (>20 cells affected) (Fig. 10). Scanning electron microscopic evaluations of the epidermal-dermal junction showed typical areas of epidermal-dermal separation. The epidermis with an intact stratum corneum had been lifted from the dermis (Fig. 11). Dermal papilla were noted and focal areas of attachment and separation were seen. TEM showed that separation occurred between the lamina densa and lamina lucida of the basement membrane. Evaluation of the space between the separation showed an amorphous substance containing cytoplasmic remnants of organelles (Fig. 12). Pyknosis was more severe than in any other of the HD-treated IPPSFs but was restricted to the stratum basale and stratum spinosum cell layers (Fig. 13). In addition, there were dyskeratotic and karyolytic basal cells, large cytoplasmic vacuoles, and dilated rough endoplasmic reticulum.

DISCUSSION

A major concern in cutaneous vesicant research has been the inability to identify an in vivo or in vitro model that possesses a cutaneous tissue that is structurally and functionally similar to human skin and able to produce the characteristic gross skin lesions typical of human exposure to HD. Historically, vesicles or vesicle-like lesions have been produced with HD in many diverse animal models, including bird skin, frog skin, canine mammary gland skin, rabbit ear skin, and thermally burned reepithelialized guinea pig skin (Renshaw, 1946). Microvesicles have been elicited with HD in the rabbit and guinea pig (Vogt et al., 1984), hairless guinea pig (Marlow et al., 1990; Mershon et al., 1990; Petrali et al., 1990), and the human skin grafted athymic nude mouse model (McGown et al., 1987; Papirmeister et al., 1984a,b). However, microvesicles have been described in pigs treated topically with neat butyl mustard (Westrom, 1987) as well as with HD and L, but no gross lesions were noticed (Mitcheltree et al., 1989). The in vitro full-thickness human skin organ culture model exposed to HD developed microscopic epidermal-dermal separation (Mol et al., 1991). However, no macroscopic blisters typical of human exposure have been reported in any of these models (Requena et al., 1988; Willems, 1989).

Previous studies have utilized the IPPSF to biochemically and morphologically assess the dermatotoxicity of the monofunctional HD analogue CEMS (King and Monteiro-Riviere, 1990) and the potent organic arsenical L (King and Monteiro-Riviere, 1992). In these studies, distinct changes occurred as a result of topical exposure to CEMS and L. Morphological changes included the formation of gross blisters, microscopic vesicles, and extensive basal cell pyknosis. TEM revealed EDJ separation between the lamina lucida and lamina densa, intracellular vacuolization, and mitochondrial swelling.

Although the IPPSF's toxicologic profile for vesicants is similar to that seen after CEMS application (King and Monteiro-Riviere, 1990), it was significantly differ-

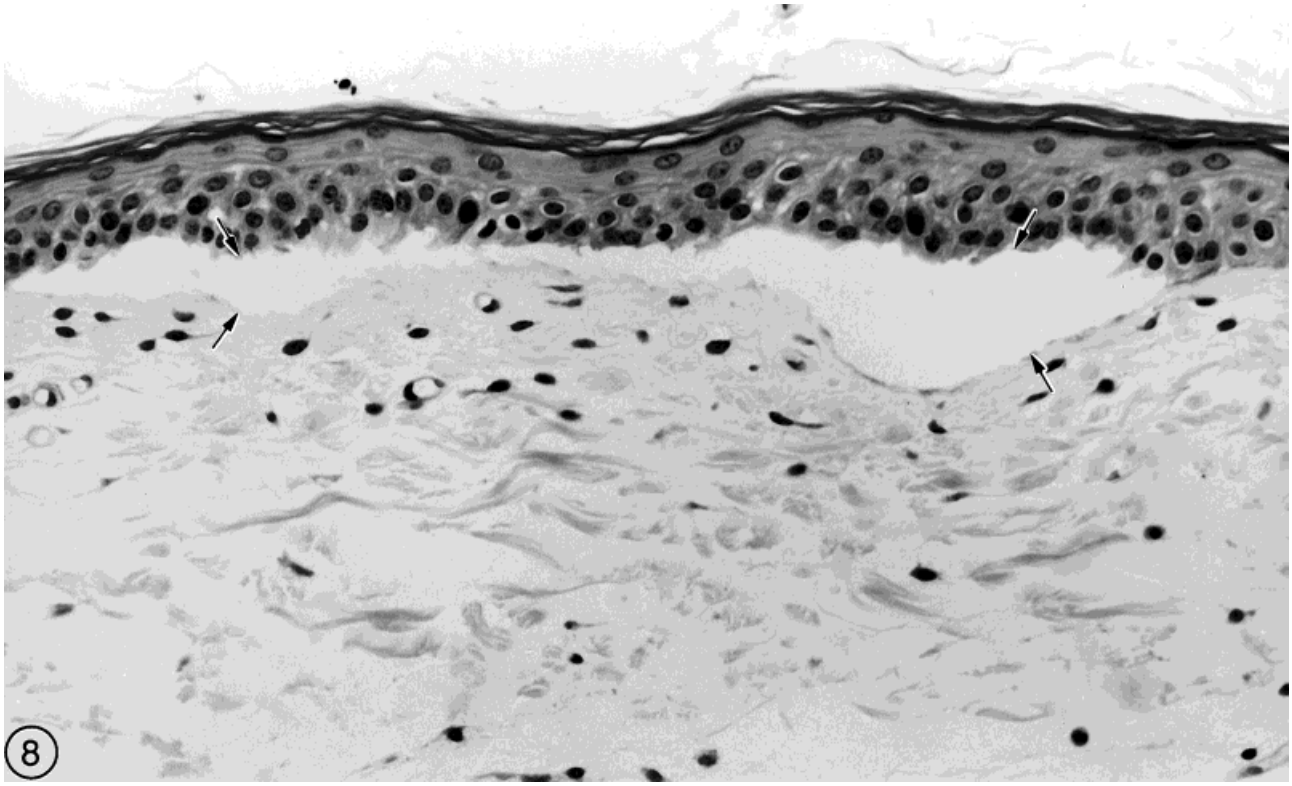

Fig. 8. LM of a 5.0 mg/ml of HD-treated IPPSF exhibiting focal epidermal-dermal separation (arrows). ×350.

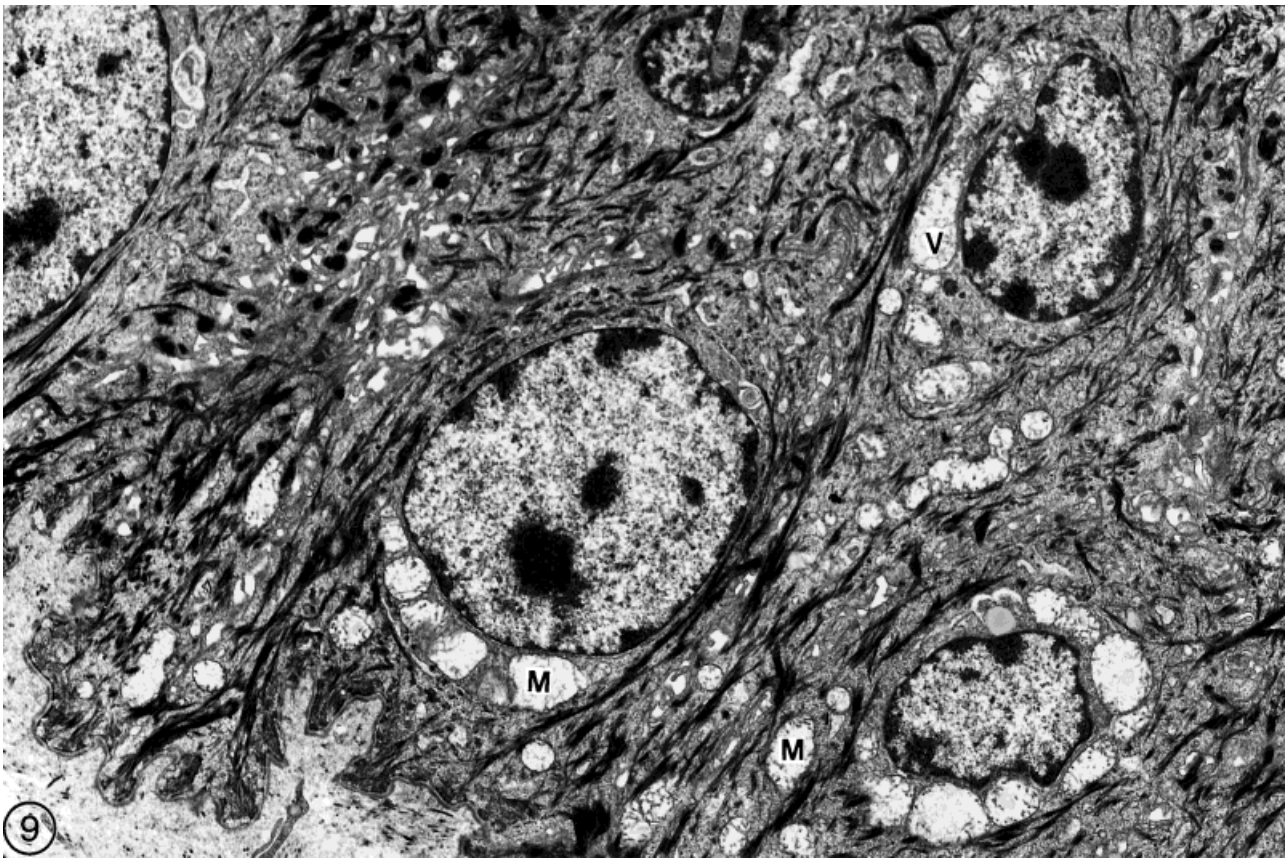

Fig. 9. TEM of a 5.0 mg/ml of HD-treated IPPSF showing stratum basale cells. Note the swollen mitochondria (M) which eventually coalesce to form large vacuoles (V). ×7,200.

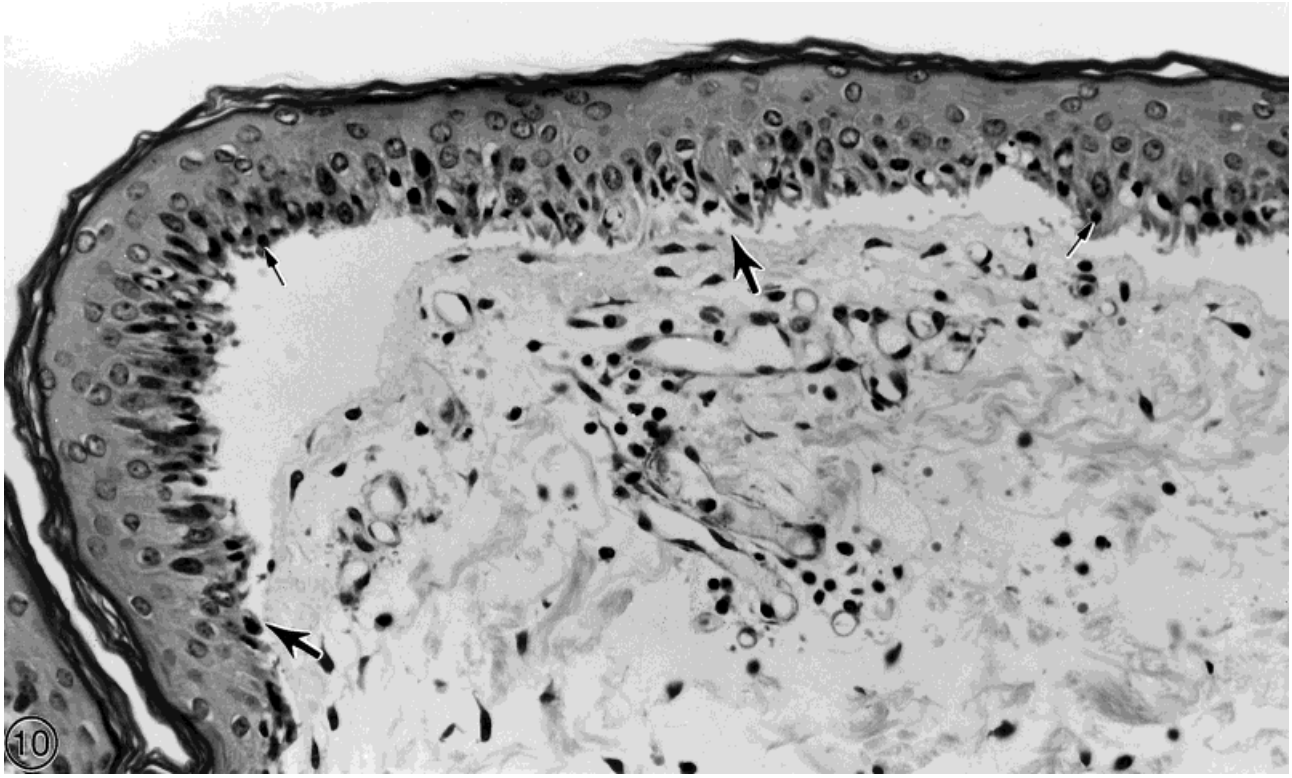

Fig. 10. LM of a 10.0 mg/ml of HD-treated IPPSF depicting epidermal-dermal separation (large arrows) and pyknotic basal cells (small arrows). ×500.

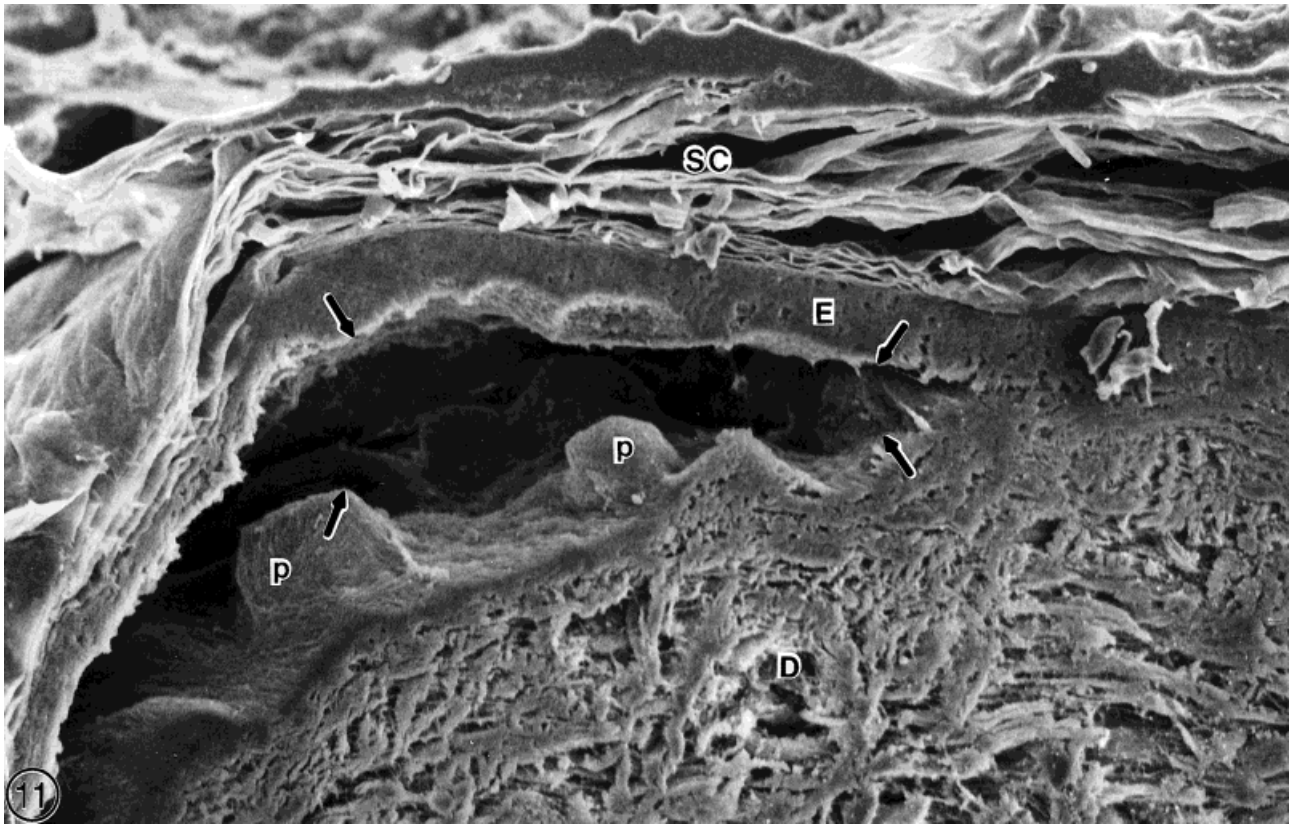

Fig. 11. SEM of a 10.0 mg/ml of HD-treated IPPSF showing a large separation (arrows) occurring between the epidermis (E) and dermis (D). Note the stratum corneum (SC) and dermal papilla (p) are present. ×275.

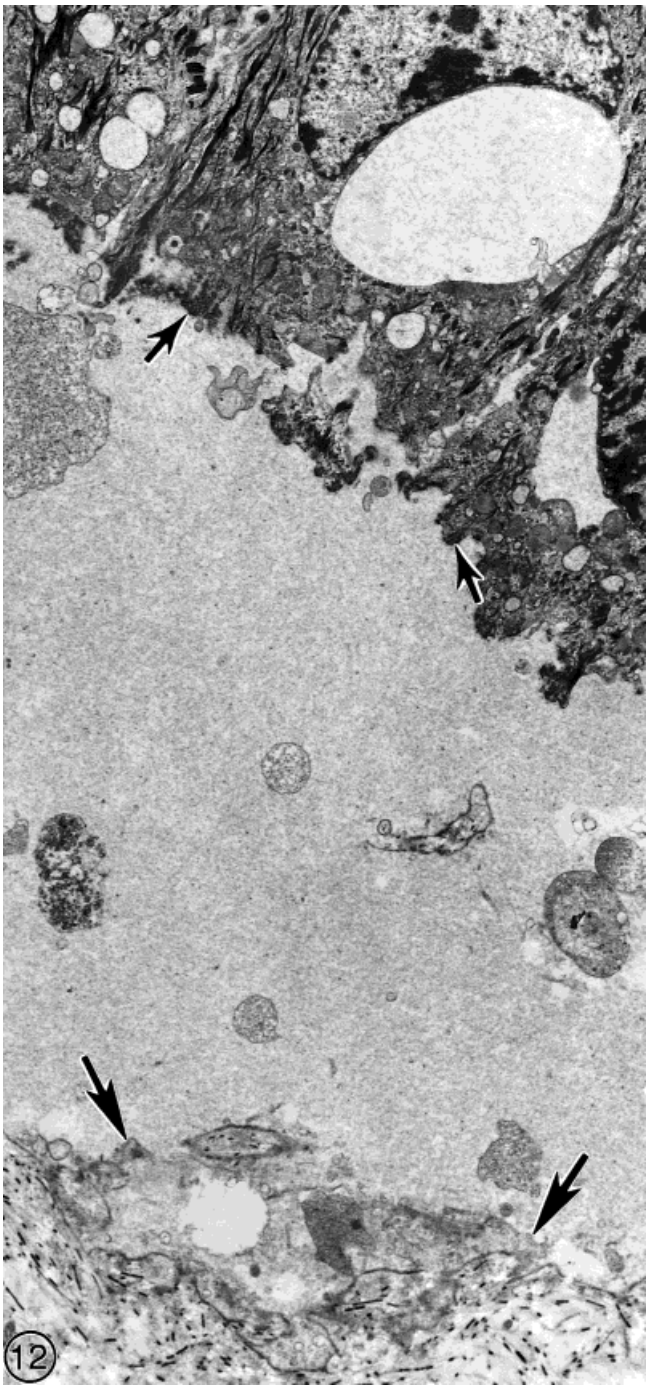

Fig. 12. TEM of a 10.0 mg/ml of HD-treated IPPSF depicting that the epidermal-dermal separation occurred between the lamina lucida (small arrows) and lamina densa (large arrows). ×5,500.

ent from that seen after vehicle treatment (King and Monteiro-Riviere, 1991), strong acids and alkali (Srikrishna and Monteiro-Riviere, 1991), lidocaine iontophoresis (Monteiro-Riviere, 1990b), or paraquat (Srikrishna et al., 1992). In each of these cases, toxicity was manifested by compound-specific morphological alterations and changes (or lack of change) in VR and GU. These findings thus lend credence to pathophysiological interpretations made from the IPPSF data.

The biochemical changes that occurred agree with studies reported by other investigators. Most studies associate a decrease in GU and an inhibition of glycolysis as hallmarks of HD-induced vesication (Bernstein et al., 1987; Gray, 1989; Mol et al., 1991; Papirmeister et al., 1985). To support this, treatment of IPPSFs with neat CEMS and L resulted in a dramatic decrease in CGU (King and Monteiro-Riviere, 1990; King et al., 1992). HD even decreased GU in the absence of gross blister formation, suggesting that the magnitude of this effect may correlate with the occurrence of vesication. However, these findings strongly link decreased glucose metabolism with vesication.

Other workers believe that changes in vascular permeability directly resulting from HD action at the microvasculature are involved in the pathogenesis of HD-induced blisters (Dannenberg et al., 1985; Harada et al., 1985, 1987; Higuchi et al., 1988; Vogt et al., 1984). This hypothesis was supported in our studies, since changes in VR are an early event associated with HD treatment. The increased VR suggested that HD induced vasodilation and increased capillary permeability, which resulted in edema and perfusion resistance. It is possible that a combination of decreased GU and increased capillary permeability results in vesication. It is important to note that L-induced vesication is associated with less severe changes in both GU and VR, suggesting a different pathogenesis (King et al., 1992). This different profile also supports the specificity of the observed HD-induced changes.

Gross and microscopic observations did show a correlation of dose concentration to blister and microvesicle formation. The blisters were similar to those found in HD-exposed human skin (Requena et al., 1988; Willems, 1989). Morphological observations include epidermal-dermal separation, intracellular and intercellular epidermal edema, and pyknotic nuclei. Microvesicles were caused by EDJ separation at the level of the lamina lucida. The focal distribution of the lesions observed in our study may reflect the cell-cycle specificity of epidermal basal cells to HD-induced DNA toxicity and/or be due to uneven agent absorption in the skin. Also, this is supported by the heterogeneous pattern of dark basal cell formation. This delay in blister formation is characteristic of HD vesication.

The observed events in the pathogenesis of HD-induced vesication has implications on the validity of a number of hypotheses presently in the literature. Papirmeister et al. (1991) presents a monograph outlining the following theories: 1) the poly (ADP-ribose) polymerase (PADPRP) hypothesis, which links HD vesication with HD alkylation of DNA, followed by polymerase activation, cellular NAD^+ depletion, inhibition of glycolysis, and pathology (Papirmeister et al., 1985); 2) the thiol-Ca^{2+} hypothesis, which postulates a primary effect of HD-induced reduction in cellular protein thiol levels, glutathione depletion, increased intracellular Ca^{2+} concentration, disrupted cytoarchitecture, and ultimately cell death; 3) the lipid peroxidation hypothesis, which suggests HD-induced glutathione depletion results in increased levels of toxic lipid peroxides and ultimately in irreversible membrane damage (Papirmeister et al., 1991); and 4) a combination which links all of the above hypotheses.

The data generated in this study are consistent with a combination of the PADPRP and one of the oxidation

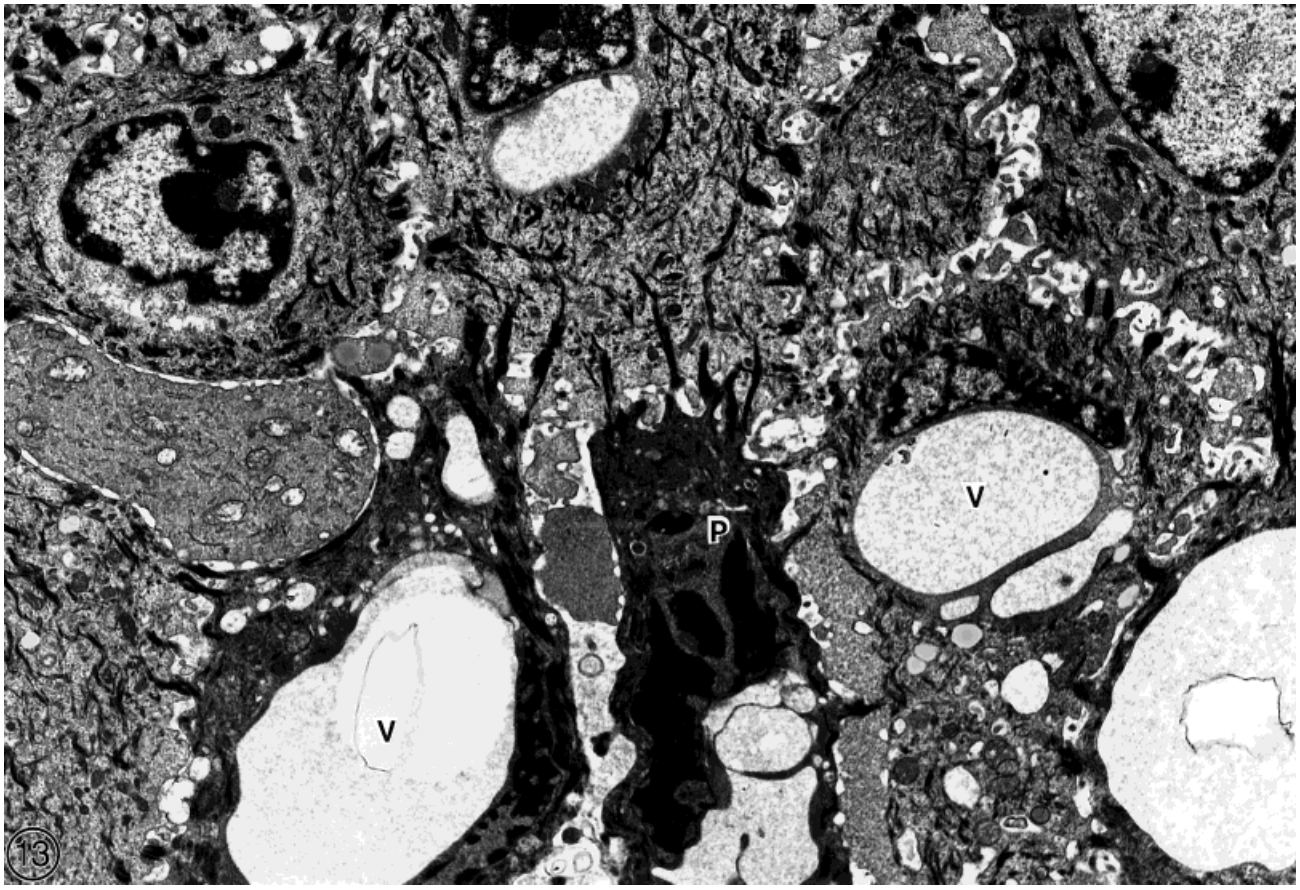

Fig. 13. TEM of a 10.0 mg/ml of HD-treated IPPSF showing typical pyknotic basale cells (P) and large cytoplasmic vacuoles (V). ×7,200.

hypotheses. The changes in nuclear structure seen at lower doses support a primary effect on DNA. The IPPSF studies clearly show that the morphological and biochemical changes are present before microvesication occurs. Acids and alkali applied to the IPPSF produce severe cellular damage without vesication (Srikrishna and Monteiro-Riviere, 1991).

Another alteration which warrants more discussion is the nuclear changes seen with HD in the IPPSF. The phenomenon of nucleolar margination and pleomorphism, which is seen in normal IPPSFs, is reflective of protein synthesis secondary to the wound healing resulting from the surgical procedure (Monteiro-Riviere et al., 1987). This is not a degenerative change because other organelles within these cells appear normal. In contrast, nucleolar segregation seen with exposure to HD and L, and not seen in control IPPSFs, signifies cellular injury. It has been postulated that nucleolar segregation probably reflects toxicant binding to DNA and inhibition of DNA-dependent RNA synthesis. This has been observed in a variety of tissues in response to agents that inhibit RNA synthesis, including chemical carcinogens (Goldblatt and Sullivan, 1970; Shinozuka, 1972; Svobada and Higginson, 1968; Svoboda and Reddy, 1975) in respiratory epithelium in response to benzo(a) pyrene-ferric oxide exposure (Harris et al., 1971), and to formaldehyde (Monteiro-Riviere and Popp, 1986). This lesion develops in response to the reduction of RNA synthesis when the biochemical block is at the level of RNA polymerase or DNA. In addition, it is known that HD alkylates DNA (Fox and Scott, 1980). Therefore, nucleolar segregation may be the morphological sequelae of mustard binding to DNA and may serve as a useful biomarker of HD effect in experimental studies.

In summary, it is evident that the pathogenesis of HD-induced vesication is a multifaceted process which is associated with DNA damage and general cytotoxicity. The IPPSF appears to be a relevant model since the morphological appearance and the biochemical and physiological effects are very similar to that reported in humans. Importantly, gross blisters also form in this in vitro model. The major advantage of the IPPSF, in addition to the similarity to human lesions, is that the experimental factors designed to address specific points in proposed mechanisms of HD vesication can be addressed in a biologically relevant preparation.

ACKNOWLEDGMENTS

The authors thank Rick Rogers, Rhonda Sanders, Lillian Kidd, and Jeffrey Crews for their technical assistance. This work was supported by the U.S. Army Medical Research and Development Command under contract DAMD17-87-C-7139. The views, opinions, and/or findings contained in this manuscript are those of the authors and should not be construed as an official

Department of the Army position, policy, or decision unless so designated by other documentation.

In conducting research using animals, the investigators adhered to the *Guide for the Care and Use of Laboratory Animals*, prepared by the Committee on Care and Use of Laboratory Animals of the Institute of Laboratory Animal Resources, National Research Council (NIH publication 86-23, revised 1985).

REFERENCES

Bartek, M.J., LaBudde, J.A., and Maibach, H.I. (1972) Skin permeability in vivo: Comparison in rat, rabbit, pig, and man. J. Invest. Dermatol., 58:114–123.

Bernstein, I.A., Brabec, M.J., Conolly, R.C., Gray, R.H., and Kulkarn, A. (1987) Chemical blistering: Cellular and macromolecular components. USAMRDC: Annual Report AD-A190 313. pp. 1–34.

Bowman, K.F., Monteiro-Riviere, N.A., and Riviere, J.E. (1991) Development of surgical techniques for preparation of in vitro isolated perfused porcine skin flaps for percutaneous absorption studies. Am. J. Vet. Res., 52:75–82.

Carver, M.P., Williams, P.L., and Riviere, J.E. (1989) The isolated perfused porcine skin flap (IPPSF). III. Percutaneous absorption pharmacokinetics of organophosphates, steroids, benzoic acid and caffeine. Toxicol. Appl. Pharmacol., 97:324–337.

Dannenberg, A.M., Jr., Pula, P.J., Liu, L.H., Harada, S., Tanaka, F., Vogt, R.F., Jr., Kajiki, A., and Higuchi, K. (1985) Inflammatory mediator and modulators released in organ culture from rabbit skin lesions produced in vivo by sulfur mustard. I. Quantitative histopathology, PMN, basophil, and mononuclear cell survival, and unbound (serum) protein content. Am. J. Pathol., 121:15–27.

Fox, M., and Scott, D. (1980) The genetic toxicology of nitrogen and sulphur mustard. Mutat. Res., 75:131–168.

Goldblatt, P.J., and Sullivan, R.J. (1970) Sequential morphological alterations in hepatic cell nucleoli induced by various doses of actinomycin D. Cancer Res., 30:1349–1356.

Gray, P.J. (1989) A Literature Review on the Mechanism of Action of Sulfur and Nitrogen Mustard. USAMRDC Report MRL-TR-89-24.

Harada, S., Dannenberg, A.M., Jr., Kajiki, A., Higuchi, K., Tanaka, F., and Pula, P.J. (1985) Inflammatory mediators and modulators released in organ culture from rabbit skin lesions produced in vivo by sulfur mustard. II. Evans blue dye experiments that determined the rates of entry and turnover of serum protein in developing and healing lesions. Am. J. Pathol., 121:28–38.

Harada, S., Dannenberg, A.M., Jr., Vogt, R.F., Jr., Myrick, J.E., Tanaka, F., Redding, L.C., Merkhofer, R.M., Pula, P.J., and Scott, A.L. (1987) Inflammatory mediators and modulators released in organ culture from rabbit skin lesions produced in vivo by sulfur mustard. III. Electrophoretic protein fractions, trypsin-inhibitory capacity, α_1-proteinase inhibitor, and α_1- and α_2-macroglobulin proteinase inhibitors of culture fluids and serum. Am. J. Pathol., 126:148–163.

Harris, C.C., Sporn, M.B., Kaufman, D.G., Smith, J.M., and Baker, M.S. (1971) Acute ultrastructural effects of benzo(a)pyrine and ferric oxide on the hamster tracheobronchial epithelium. Cancer Res., 31:1977–1989.

Higuchi, K., Kajiki, A., Nakamura, M., Liu, L.H., Harada, S., Pula, P.J., Scott, A.L., and Dannenberg, A.M., Jr. (1988) Proteases released in organ culture by acute dermal inflammatory lesions produced in vivo in rabbit skin by sulfur mustard: Hydrolysis of synthetic peptide substrates for trypsin-like and chymotrypsin-like enzymes. Inflammation, 12:311–334.

King, J.R., and Monteiro-Riviere, N.A. (1990) Cutaneous toxicity of 2-chloroethyl methyl sulfide in isolated perfused porcine skin. Toxicol. Appl. Pharmacol., 104:167–179.

King, J.R., and Monteiro-Riviere, N.A. (1991) Effects of organic solvent vehicles on the viability and morphology of isolated perfused porcine skin. Toxicology, 69:11–26.

King, J.R., Riviere, J.E., and Monteiro-Riviere, N.A. (1992) Characterization of lewisite toxicity in isolated perfused skin. Toxicol. Appl. Pharmacol., 116:189–201.

Marlow, D.D., Mershon, M.M., Mitcheltree, L.W., Petrali, J.P., and Jaax, G.P. (1990) Sulfur mustard–induced skin injury in hairless guinea pigs. J. Toxicol. Cut. Ocular Toxicol., 9:179–192.

McDowell, E.M., and Trump, B.F. (1976) Histologic fixatives suitable for diagnostic light and electron microscopy. Arch. Pathol. Lab. Med., 100:404–414.

McGown, E.L., Van Ravenswaay, T., and Dumlao, C.R. (1987) Histologic changes in nude mouse skin and human skin xenografts following exposure to sulfhydryl reagents: Arsenicals. Toxicol. Pathol., 15:149–156.

Mershon, M.M., Mitcheltree, L.W., Petrali, J.P., Braue, E.H., and Wade, J.V. (1990) Hairless guinea pig bioassay model for vesicant vapor exposures. Fundam. Appl. Toxicol., 15:622–630.

Mitcheltree, L.W., Mershon, M.M., Wall, H.G., Pulliam, J.D., and Manthei, J.H. (1989) Microblister formation in vesicant-exposed pig skin. J. Toxicol. Cut. Ocular Toxicol., 8:309–319.

Mol, M.A.E., De Vries, R., and Kluivers, A.W. (1991) Effects of nicotinamide on biochemical changes and microblistering induced by sulfur mustard in human skin organ cultures. Toxicol. Appl. Pharmacol., 107:439–449.

Monteiro-Riviere, N.A. (1990a) Specialized technique: Isolated perfused porcine skin flap. In: Methods for Skin Absorption. B.W. Kemppainen and W.G. Reifenrath, eds. CRC Press, Boca Raton, FL, pp. 175–189.

Monteiro-Riviere, N.A. (1990b) Altered epidermal morphology secondary to lidocaine iontophoresis: In vitro and in vivo studies in porcine skin. Fundam. Appl. Toxicol., 15:174–185.

Monteiro-Riviere, N.A., and Manning, T.O. (1987) The effects of different fixatives on the porcine integument. In: 45th Annual Proceedings, Electron Microscopy Society of America, G.W. Bailey ed. San Francisco Press, San Francisco, pp. 948–949.

Monteiro-Riviere, N.A., and Popp, J.A. (1986) Ultrastructural evaluation of acute nasal toxicity in the rat respiratory epithelium in response to formaldehyde gas. Fundam. Appl. Toxicol., 6:251–262.

Monteiro-Riviere, N.A., Bowman, K.L., Scheidt, V.J., and Riviere, J.E. (1987) The isolated perfused porcine skin flap (IPPSF). II. Ultrastructural and histological characterization of epidermal viability. In Vitro Toxicol., 1:241–252.

Papirmeister, B., Gross, C.L., Petrali, J.P., and Hixson, C.J. (1984a) Pathology produced by sulfur mustard in human skin grafts on athymic nude mice. I. Gross and light microscopic changes. J. Toxicol. Cut. Ocular Toxicol., 3:371–391.

Papirmeister, B., Gross, C.L., Petrali, J.P., and Meier, H.L. (1984b) Pathology produced by sulfur mustard in human skin grafts on athymic nude mice. II. Ultrastructural changes. J. Toxicol. Cut. Ocular Toxicol., 3:393–408.

Papirmeister, B., Gross, C.L., Meier, H.L., Petrali, J.P., and Johnson, J.B. (1985) Molecular basis for mustard-induced vesication. Fundam. Appl. Toxicol., 5:S134–S149.

Papirmeister, B., Feister, A.J., Robinson, S.I., and Ford, R.D. (1991) In: Medical Defense Against Mustard Gas: Toxic Mechanisms and Pharmacological Implications, CRC Press, Boca Raton, FL.

Petrali, J.P., Oglesby, S.B., and Mills, K.R. (1990) Ultrastructure correlates of sulfur mustard toxicity. J. Toxicol. Cut. Ocular Toxicol., 9:193–214.

Reifenrath, W.G., Chellquist, E.M., Shipwash, E.A., and Jederberg, W.W. (1984a) Evaluation of animal models for predicting skin penetration in man. Fundam. Appl. Toxicol., 4:S224–S230.

Reifenrath, W.G., Chellquist, E.M., Shipwash, E.A., Jederberg, W.W., and Krueger, G.G. (1984b) Percutaneous penetration in the hairless dog, weanling pig and grafted athymic nude mouse: Evaluation of models for predicting skin penetration in man. Br. J. Dermatol., 11:123–135.

Renshaw, B. (1946) Mechanisms in production of cutaneous injuries by sulfur and nitrogen mustards. In: Chemical Warfare Agents and Related Chemical Problems, Vol. 1. Technical summary report of Division 9, National Defense Research Committee. Washington, DC, pp. 479–478.

Requena, L., Requena, C., Sanchez, M., Jaqueti, G., Aguilar, A., Sánchez-Yus, E., and Hernández-Moro, B. (1988) Chemical warfare: Cutaneous lesions from mustard gas. J. Am. Acad. Dermatol., 19:529–536.

Riviere, J.E., and Monteiro-Riviere, N.A. (1991) The isolated perfused porcine skin flap as an in vitro model for percutaneous absorption and cutaneous toxicology. CRC Crit. Rev. Toxicol., 21:329–344.

Riviere, J.E., Bowman, K.F., Monteiro-Riviere, N.A., Carver, M.P., and Dix, L.P. (1986) The isolated perfused porcine skin flap (IPPSF). I. A novel in vitro model for percutaneous absorption and cutaneous toxicology studies. Fundam. Appl. Toxicol., 7:444–453.

Riviere, J.E., Bowman, K.F., and Monteiro-Riviere, N.A. (1987) On the definition of viability in isolated perfused skin preparation. Br. J. Dermatol., 116:739–741.

Riviere, J.E., Sage, B.S., and Williams, P.L. (1991) The effects of vasoactive drugs on transdermal lidocaine iontophoresis. J. Pharm. Sci., 80:615–620.

Shinozuka, H. (1972) Response of nucleus and nucleolus to inhibition of RNA synthesis. In: The Pathology of Transcription and Translation. E. Farber, ed. Dekker, New York, p. 73–103.

Srikrishna, V., and Monteiro-Riviere, N.A. (1991) The effects of sodium

hydroxide and hydrochloric acid on the isolated perfused porcine skin flap. In Vitro Toxicol., 4:207–215.
Srikrishna, V., Riviere, J.E., and Monteiro-Riviere, N.A. (1992) Cutaneous toxicity and absorption of paraquat in porcine skin. Toxicol. Appl. Pharmacol., 115:89–97.
Svoboda, D., and Higginson, J. (1968) A comparison of ultrastructural changes in rat liver due to chemical carcinogens. Cancer Res., 28:1703–1733.
Svoboda, D., and Reddy, J. (1975) Some effects of chemical carcinogens on cell organelles. In: Cancer. F.F. Becker, ed. Plenum, New York, p. 289–295.
Vogt, R.F., Jr., Dannenberg, A.M., Jr., Schofield, B.H., Hynes, N.A., and Papirmeister, B. (1984) Pathogenesis of skin lesions caused by sulfur mustard. Fundam. Appl. Toxicol., 4:S71–S83.
Wester, R.C., and Maibach, H.I. (1985) Animal models for percutaneous absorption. In: Models in Dermatology, Vol. 2. H.I. Maibach, and N.J. Lowe, eds. Karger, Basel, pp. 159–169.
Westrom, D.R. (1987) Animal models for vesicant-induced injury. In: Proceedings of the Vesicant Workshop, February, 1987. U.S. Army Medical Research Institute of Chemical Defense, Aberdeen Proving Ground, MD, pp. 91–96.
Willems, J.L. (1989) Clinical management of mustard gas casualties. Annales Medicine Militaris Belgicae, 3:1–61.
Williams, P.L., Carver, M.P., and Riviere, J.E. (1990) A physiologically relevant pharmacokinetic model of xenobiotic percutaneous absorption utilizing the isolated perfused porcine skin flap (IPPSF). J. Pharm. Sci., 79:305–311.